CHEMISTRY
A EUROPEAN JOURNAL

DOI: 10.1002/chem.201000427

VIP

Electroactive Benzothiazole Hydrazones and Their $[Mo_6O_{19}]^{2-}$ Derivatives: Promising Building Blocks for Conducting Molecular Materials

Sylvain Gatard,[a] Sébastien Blanchard,*[a] Bernd Schollhorn,[c] Pierre Gouzerh,[a] Anna Proust,[a, b] and Kamal Boubekeur*[a]

Abstract: The electroactive benzothiazole hydrazone AMBTH–H_2, a new member of the 2,2′-azino-bis(*N*-alkylbenzothiazole) family, was synthesised in a five-step procedure and characterised by using X-ray diffraction along with two intermediates and the *N*-methylbenzothiazole hydrazone MBTH–H_2. Both AMBTH–H_2 and MBTH–H_2 were coupled to $[Mo_6O_{19}]^{2-}$ in acetonitrile in the presence of dicyclohexylcarbodiimide and dimethylaminopyridine to give two new diazoalkane–hexamolybdates, which were isolated as tetrabutylammonium salts and characterised by using IR, UV/Vis and NMR spectroscopies, cyclic voltammetry and, for one of them, X-ray diffraction. The packing arrangement molecules in crystals of AMBTH–H_2, the redox features of the AMBTH–hexamolybdate hybrid together with a good electronic communication between the organic π system and the molybdenum centres make these compounds very promising blocks for the synthesis of conducting molecular materials.

Keywords: conducting materials · organic donors · organic–inorganic hybrid composites · polyoxometalates · X-ray diffraction

Introduction

Multifunctional materials are a challenging synthetic target in contemporary chemistry.[1,2] One promising way to reach such a target is the bottom-up molecular approach in which different properties are associated through two different molecular networks, such as cationic and anionic sublattices. It allows the coexistence in the material of distinct physical properties, such as conduction,[3–5] chirality,[4,6] luminescence,[7] magnetism,[6–9] and/or spin cross-over.[3,10] Provided that the interactions between these properties (or networks) are strong enough, it may also lead to enhanced or even new properties, as observed for example in the case of the magnetochiral effect.[11]

Among these various materials, magnetic molecular conductors have been extensively studied.[5,12] Although a wide diversity of anions has been used to provide magnetic properties, the conducting component often relies on radical cations derived from the tetrachalcogenofulvalenes, and more scarcely on the relatively unstable dithiadiazafulvalene.[13] Inspired by the pioneering works of Hünig et al.[14] and then Wheland,[15] some of us have started to explore the chemistry of 2,2′-azino-bis(*N*-alkylbenzothiazole) derivatives as an alternative donor. Thus, using the electrocrystallisation technique[16] with commercially available 2,2′-azino-bis(3-ethylbenzothiazole-6-sulfonate) ($ABTS^{2-}$) and various cations, hybrid organic-inorganic molecular materials have been synthesised.[17–19] Recently, some interesting results on the electrocrystallisation of a selenium analogue, 2,2′-azino-bis(3-methylbenzoselenazole), have been reported.[20]

Polyoxometalates (POMs) are early transition-metal oxo clusters.[21,22] Owing to their diversity in terms of molecular structures and properties, they have been widely used as building blocks in molecular materials.[23–27] Intensive research on molecular conductors with integrated POMs has been developed by several groups[28,29] and a few examples of metallic behaviour have been reported.[30] Yet, synergetic

[a] Dr. S. Gatard, Dr. S. Blanchard, Prof. P. Gouzerh, Prof. A. Proust, Prof. K. Boubekeur
Institut Parisien de Chimie Moléculaire
UMR CNRS 7201, UPMC Université Paris 06
Case courrier 42, 4 place Jussieu, 75252 Paris Cedex 05 (France)
Fax: (+33) 1-44-27-38-41
E-mail: sebastien.blanchard@upmc.fr
kamal.boubekeur@upmc.fr

[b] Prof. A. Proust
Institut Universitaire de France
103, bd. Saint-Michel, 75005 Paris (France)

[c] Prof. B. Schollhorn
Laboratoire d'Electrochimie Moléculaire
UMR CNRS 7591, Université Paris Diderot Paris 7
Bâtiment Lavoisier, Case 7107
15 rue Jean-Antoine de Baïf, 75205 Paris Cedex 13 (France)

Supporting information for this article is available on the WWW under http://dx.doi.org/10.1002/chem.201000427.

interactions between the anionic sublattice and the cationic sublattice at the origin of the conducting properties remain to be proved.[31] POMs are easily functionalised[32] and their organic derivatives have found applications in the implementation of covalent POM-based materials,[33–38] a class of materials that is rapidly expanding. For example, nitrogeneous derivatives have allowed the synthesis of organic-inorganic hybrids with potentially strong d–π interactions.[39] This prompted us to revisit the field of POM-based molecular conductors by looking for a covalent link between a potential organic donor and POMs.

Herein, we will first describe the synthesis of AMBTH–H_2, a new member of the 2,2′-azino-bis(*N*-alkylbenzothiazole) family, modified so that a pendant hydrazone functionality is available for further derivatisation. The rationale for designing this molecule was to keep the redox properties associated with the AMBT donor, while providing a reactive organic function capable of establishing a covalent link with the inorganic counterpart, thus enhancing electronic communication between the two components of the hybrid. We will thus describe how, modifying Peng's procedure for the functionalisation of the hexamolybdate with amine,[40] this hydrazone and the shorter analogue *N*-methylbenzothiazole hydrazone (MBTH–H_2) have been successfully coupled to the $[Mo_6O_{19}]^{2-}$ isopolyanion. The resulting organic–inorganic hybrids, which have been fully characterised, are only the second and third examples of diazoalkane POM derivatives in the literature,[41] and are promising candidates for the electrosynthesis of molecular materials with strong (covalent) interactions between the anionic (functionalised POM) and the cationic (2,2′-azino-bis(*N*-alkylbenzothiazole) organic radical) components.

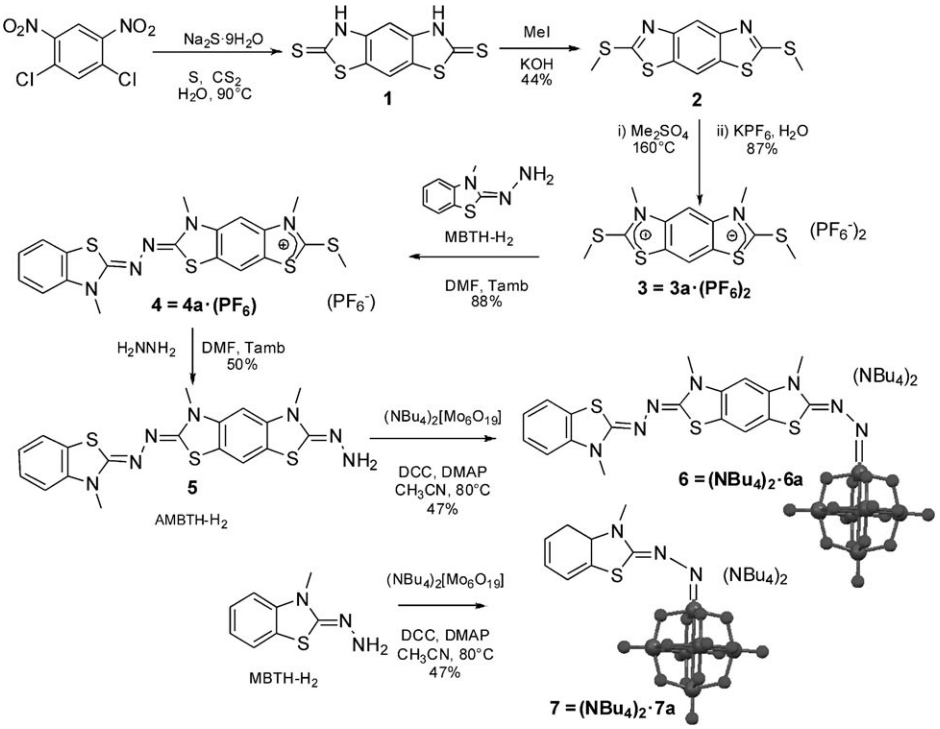

Scheme 1. Synthesis of $(NBu_4)_2[Mo_6O_{18}(AMBTH)]$ and $(NBu_4)_2[Mo_6O_{18}(MBTH)]$. (Ball and stick representation of the polyoxometallic part).

Results and Discussion

Organic precursors

Syntheses: As displayed in Scheme 1, AMBTH–H_2 (**5**) was synthesised in five steps from the commercial 1,3-dichloro-4,6-dinitrobenzene. Cyclisation in the presence of sulfur, sodium sulfide and carbone disulfide led to the corresponding dithione **1** in quantitative yield, which was subsequently alkylated on both sulfurs using methyl iodide, according to procedures described by Grandolini.[42] Recrystallisation of the resulting compound (**2**) in DMF led to yellow-orange needles, which were characterised by single-crystal X-ray diffraction. The poorly soluble **2** was further reacted with dimethylsulfate to form **3** in good yields by using a solvothermal procedure previously described by Manecke and Kautz,[43] modified such that the product was precipitated by using KPF_6 instead of $KClO_4$, to avoid the potentially hazardous perchlorate salts. Its ^1H and ^{13}C NMR spectra display, respectively, only four and seven signals, as expected for the symmetrical product methylated on both nitrogen positions.

Reaction of a slight excess of 2-*N*-methylbenzothiazole hydrazone (MBTH–H_2) with **3** in DMF at room temperature produced **4** (confirmed by NMR and X-ray diffraction analyses) in almost 90% yield. In particular, the ^1H NMR spectrum of this new species now displays 10 signals, among which four are attributed to the four different methyl groups of the dissymmetric molecule, in agreement with the reaction of the MBTH–H_2 with only one side of **3**.

Finally, **4** was allowed to react overnight with an excess of hydrazine, to give the targeted hydrazone AMBTH–H_2 (**5**) in 50% yield, as confirmed by ESI-MS (MH^+: m/z 428), ^1H NMR, ^{13}C NMR and X-ray diffraction analyses.

X-ray diffraction studies

Molecular structures: The crystal structures of MBTH–H_2, **2**, **4** and **5** have been determined by X-ray diffraction (Figure 1). Crystallographic data are summarised in Table 1

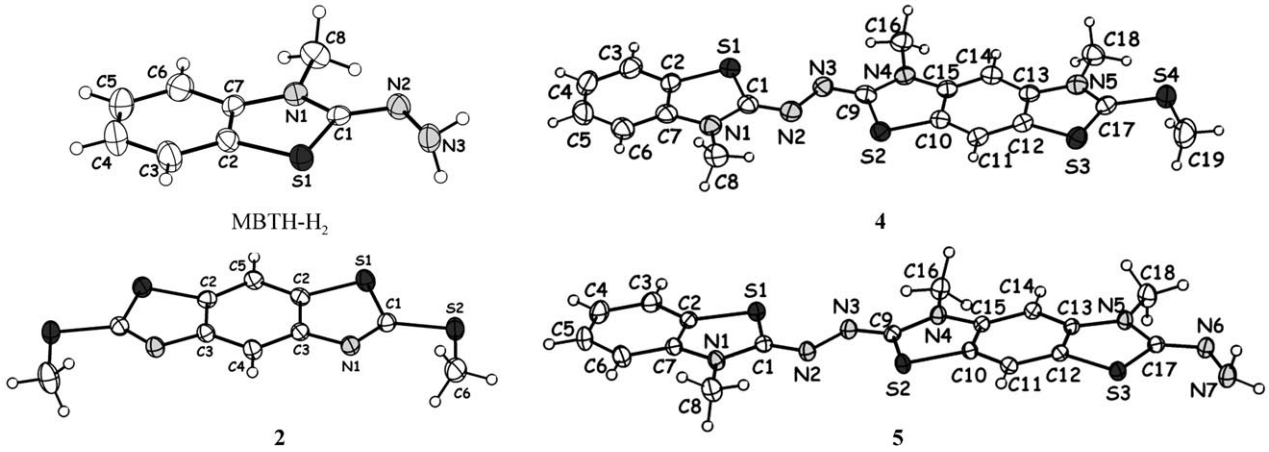

Figure 1. Molecular structures of MBTH–H_2, **2**, **4**, and **5** (ellipsoids at 50%). Though MBTH–H_2 is commercially available, its X-ray structure has not been reported before.

Table 1. Crystal data and structure refinement for MBTH-H_2, **2**, **4**, **5**, and **7**.

	MBTH–H_2	**2**	**4**	**5**	**7**
formula	$C_8H_9N_3S$	$C_{10}H_8N_2S_4$	$C_{44}H_{41}F_{12}N_{11}O_2P_2S_8$	$C_{30}H_{27}N_9O_4S_3$	$C_{40}H_{79}Mo_6N_5O_{18}S$
FW [g mol^{-1}]	179.24	284.42	1302.38	673.80	1525.78
space group	*Pbca*	*Pbca*	$P\bar{1}$	$P\bar{1}$	$P\bar{1}$
a [Å]	5.9750(8)	5.4337(5)	8.318(4)	10.4951(9)	12.1620(15)
b [Å]	8.3660(7)	11.6936(8)	11.013(4)	10.7682(12)	12.3760(13)
c [Å]	34.576(5)	19.0855(15)	15.748(9)	14.8603(14)	19.9190(18)
α [°]	90.00	90.00	79.23(4)	107.730(8)	97.568(7)
β [°]	90.00	90.00	84.15(4)	100.821(8)	92.804(12)
γ [°]	90.00	90.00	79.97(5)	92.693(6)	93.170(14)
V [Å^3]	1728.3(4)	1212.68(17)	1391.9(12)	1561.4(3)	2962.7(6)
Z	8	4	1	2	2
T [K]	293(2)	250(2)	250(2)	200(2)	250(2)
ρ calcd [g cm^{-3}]	1.378	1.558	1.554	1.433	1.710
unique reflns [$I>2\sigma(I)$]	2441/2057	2098/1417	8079/5634	9043/6039	17174/12058
no. params/restr	116/0	75/0	338/7	424/0	640/2
μ ($Mo_{K\alpha}$) [cm^{-1}]	0.319	0.754	0.467	0.29	1.332
$R1[I>2\sigma(I)]/wR2$[all data]	0.0402/01257	0.0389/0.0953	0.0669/0.1484	0.442/1.1014	0.0450/0.1203
G.O.F.	1.016	1.018	0.987	0.1204	0.949
residual density [e Å^{-3}]	0.21/−0.26	0.32/−0.31	1.02/−0.97	0.511/−0.381	0.78/−0.80

and relevant bond lengths are listed in Table 2. The molecular structures of MBTH–H_2, **4** and **5**, though determined at different temperatures, display similar N−C and C−S bond lengths (av N−C: 1.383(4), av C−S: 1.780(3) Å) for the thiazole rings bounded to an external N atom, indicating predominantly single-bond character.

For the structure of **2**, the molecule lies on a twofold crystallographic axis passing through the C4 and C5 atoms. The N1−C1 bond length shrinks to 1.303(2) Å, in agreement with the formation of a double bond within the ring upon methylation of the benzothiazole thione starting material.

Interestingly, for **4**, carbon atom C17 is only 0.004 Å above the planar thiazole ring (N5, C17, S3, C12, C13), and is clearly sp^2 hybridised. The C17−N5 bond length (1.343(6) Å) is intermediate between the single bond observed in most thiazole rings and the double bond in **2**, whereas both C−S bonds (C17−S3: 1.714(5), C17−S4:

Table 2. Selected bond lengths [Å] for MBTH-H_2, **2**, **4**, **5** and **7** and bond angle for **7**.

2	**4**	**5**	MBTH–H_2	**7**
S1−C1 1.767(2)	S1−C1 1.768(5)	S1−C1 1.780(2)	S1−C1 1.776(3)	S1−C1 1.760(5)
N1−C1 1.303(2)	N1−C1 1.381(6)	N1−C1 1.381(2)	N1−C1 1.380(4)	N1−C1 1.367(5)
S2−C1 1.757(2)	N1−C8 1.459(6)	N1−C8 1.461(2)	N1−C8 1.472(4)	N1−C8 1.473(5)
	N2−C1 1.305(6)	N2−C1 1.300(2)	N2−C1 1.294(4)	N2−C1 1.323(7)
	N2−N3 1.416(6)	N2−N3 1.422(2)	N2−N3 1.448(4)	N2−N3 1.324(5)
	N3−C9 1.302(6)	N3−C9 1.295(2)		Mo1−N3 1.773(4)
	N4−C9 1.384(6)	N4−C9 1.386(2)		
	S2−C9 1.783(5)	S2−C9 1.782(2)		Mo1-N3-N2 176.6(3)
	S3−C17 1.714(5)	S3−C17 1.785(2)		
	N5−C17 1.343(6)	N5−C17 1.384(2)		
	S4−C17 1.733(5)	N6−C17 1.290(2)		
		N6−N7 1.466(2)		

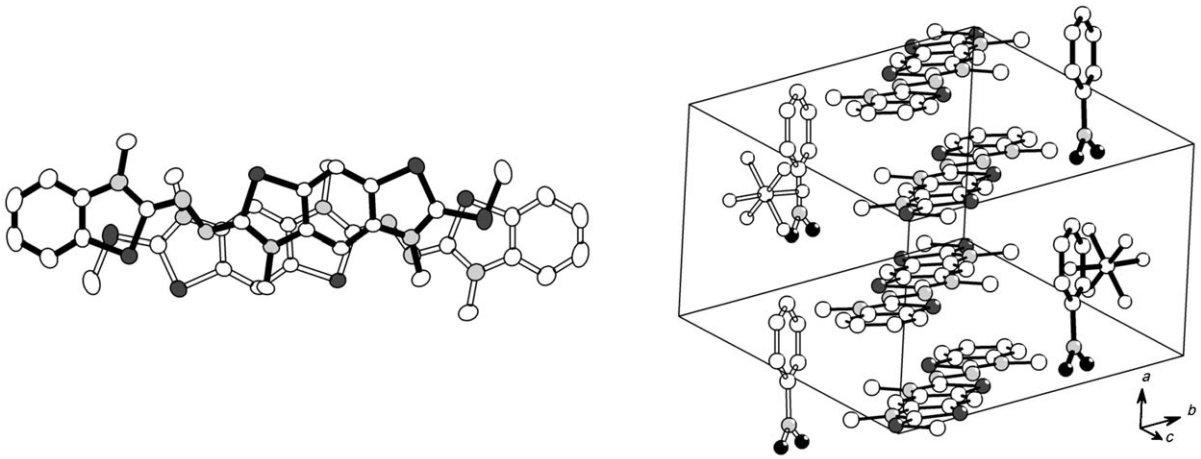

Figure 2. Packing arrangement in **4**.

1.733(5) Å) in **4** are shorter than the C–S single bonds in **2** (1.757(2) and 1.767(2) Å). All these features are in agreement with a C17-centred carbocation in **4**, delocalised over the three neighbouring heteroatoms.

Finally, the terminal N–N bonds in MBTH–H_2 (N2–N3: 1.448(4) Å) and **5** (N6–N7: 1.466(2) Å) are somewhat longer than the central N2–N3 bond lengths between thiazole rings in **4** and **5** (respectively 1.416(6) and 1.422(2) Å), showing some delocalisation of the surrounding C=N double bonds and thus electronic communication between the benzothiazole rings in **4** and **5**.

Packing arrangements: The packing arrangement of molecule **2** is described in the Supporting Information.

In compound **4**, the planar cations are uniformly π stacked approximately along the [100] direction with short plane-to-plane distance of 3.47 Å (Figure 2, for the colour version see the Supporting Information). These columns are sandwiched by mixed planes of anions and (disordered) nitrobenzene solvent molecules arising from the recrystallisation process. The planes of the cations and the nitrobenzene molecules are perpendicular. Within a column the cations are stacked in a head-to-tail fashion. This particular orientation may reflect: i) The dipolar interactions between to adjacent molecules, ii) the decrease of the coulombic repulsion by increasing the distance between the carbocations C17, and iii) the decrease of the steric contribution from the large S–Me terminal groups. Despite the absence of classic hydrogen bonds, one can note two short intermolecular C–H···F contacts, respectively linear and bifurcated, whose characteristics are given in Table 3.

Table 3. Short intermolecular contacts in **4**. (D = donor, A = acceptor).

Contact	D–H [Å]	H···A [Å]	D···A [Å]	D-H···A [°]
C3–H3···F1[a]	0.94	2.38	3.276	160
C18–H18A···F4[b]	0.97	2.49	3.171	127

[a] Symmetry code: $-1+x$, $1+y$, z. [b] Symmetry code: $1-x$, $1-y$, $1-z$.

Compound **5** (Figure 3, for the colour version see the Supporting Information) belongs to the triclinic $P\bar{1}$ space group with two stacked benzothiazole derivatives and four nitrobenzene molecules in the unit cell. The arrangement along the *c* axis is dominated by π-stacking interactions, with dimers of AMBT-H_2 separated by four molecules of nitrobenzene in a box-like arrangement. In these dimers, the two molecules are separated by approximately 3.50 Å. More-

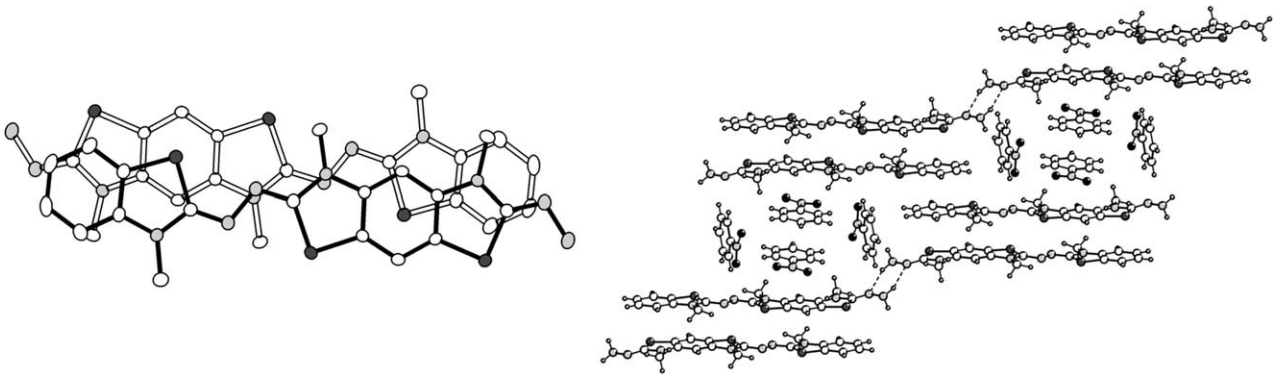

Figure 3. Packing arrangement in **5**.

over, for similar reasons as for **4**, these two molecules adopt a head-to-tail arrangement. Among the four molecules of solvent, two are stacked with a plane-to-plane distance of 3.43 Å, adopting a head-to-tail orientation, owing to dipolar interactions. This dimer of nitrobenzene is loosely sandwiched between the two other solvent molecules in a head-to-tail orientation. These dimers of solvent and of hydrazone molecules are then π stacked with a plane-to-plane mean distance of 3.40 Å. Dimers of AMBTH–H_2 in one column are linked to those in neighbouring columns through hydrogen-bonds between hydrazone groups, leading to N-N-H···N-N-H six-membered rings (Table 4).[44,45] This results in a stair like arrangement of interconnected dimers, the holes between the stairs being filled with the four solvent molecules.

Table 4. Short intermolecular contacts in **5**.

Contact	D–H [Å]	H···A [Å]	D···A [Å]	D-H···A [°]
N7–H7A ···N6[a]	0.97	2.32	3.230	156
N7–H7B···O1[b]	0.96	2.52	3.336	142

[a] Symmetry code: $-x$, $2-y$, $1-z$. [b] Symmetry code: $-1+x$, $1+y$, z.

In summary, **4** and **5** display a wide array of weak interactions (H bond, π stacking, dipole–dipole…), thus showing strong promises as building blocks for the synthesis of well-organised molecular materials.

Diazoalkane–hexamolybdates: $(NBu_4)_2[Mo_6O_{18}(AMBTH)]$ (6), $(NBu_4)_2[Mo_6O_{18}(MBTH)]$ (7)

Synthesis: Polyanions $(NBu_4)_2[Mo_6O_{18}(AMBTH)]$ [**6**: $(NBu_4)_2$-**6a**], $(NBu_4)_2[Mo_6O_{18}(MBTH)]$ [**7**: $(NBu_4)_2$-**7a**], are new members of a family of Lindqvist derivatised-hexamolybdates of the type $[Mo_6O_{18}L]^{n-}$ in which L is a nitrogenous ligand. Following the pioneering investigations by Zubieta and co-workers,[46] this family of polyanions has been extended by Errington, Maatta, Proust, Peng and Wei groups[32] and now includes nitrosyl,[47–49] hydrazido,[50] diazenido[46,51–52] nitrido[50] and imido[53–58] derivatives. One diazoalkane derivative has been also reported by Maatta and coworkers.[41] Although diazoalkane molybdenum complexes are commonly obtained by condensation of hydrazido complexes with aldehydes or ketones[59] or by reaction of low-valent molybdenum complexes with diazoalkanes,[60] diazoalkane–hexamolybdates have been prepared by metathetical exchange of oxo ligands. Thus $[Mo_6O_{18}(N_2CMeC_6H_4OMe)]^{2-}$ was obtained by reaction of $[Mo_6O_{19}]^{2-}$ with a phosphazine,[41] and polyanions **6a** and **7a** reported herein have been obtained by condensation of $[Mo_6O_{19}]^{2-}$ with the appropriate hydrazone, AMBTH–H_2 and MBTH–H_2, respectively, by using a modification of the method devised by Peng for coupling of $[Mo_6O_{19}]^{2-}$ with amines.[57] The reaction of $(NBu_4)_2[Mo_6O_{19}]$ with MBTH–H_2 in refluxing acetonitrile in the presence of dicyclohexylcarbodiimide (DCC) yielded only traces of the expected coupling product **7**. However the latter was obtained in reasonable yield (70%) when dimethylaminopyridine (DMAP) was added to the reaction mixture. Compound **6** was similarly obtained by condensation of $(NBu_4)_2[Mo_6O_{19}]$ with AMBTH-H_2 in refluxing acetonitrile in presence of DCC (1 equiv) and DMAP (0.3 equiv). Negative-mode ESI-MS investigations confirmed the identity of the products (m/z 521.7 for **7a**; m/z 645.6 for **6a**).

IR spectroscopy: The IR spectra of **6** and **7** are displayed in Figure 4, which also includes that of $(NBu_4)_2[Mo_6O_{19}]$ for comparison. The band-pattern characteristic for the Lindqvist structure clearly emerges from the low wavenumber region of the spectra (below $\tilde{\nu}=1000\ cm^{-1}$). However the ν(Mo–$O_t$) and ν(Mo-$O_b$-Mo) bands observed at $\tilde{\nu}\approx960$ and 790 cm^{-1}, split into two more or less resolved bands for **6** and **7**. (O_t and O_b mark out terminal and bridging oxo ligands, respectively). Such splittings are commonly observed in monofunctionalised hexamolybdates, for example, diazenido[52] and imido[54] derivatives.

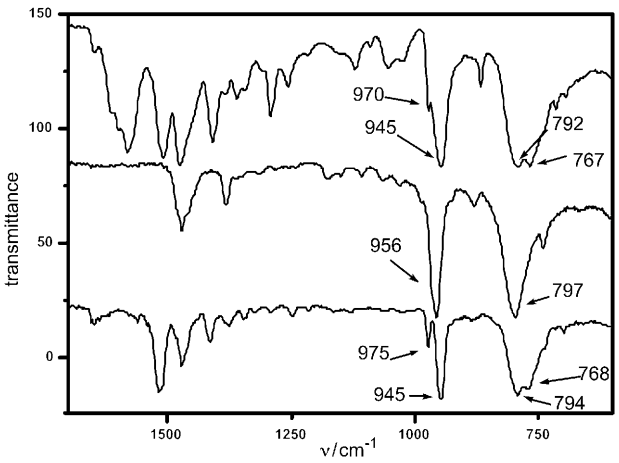

Figure 4. IR spectra of $(NBu_4)_2[Mo_6O_{18}(MBTH)]$ (bottom), $(NBu_4)_2[Mo_6O_{19}]$ (middle), and $(NBu_4)_2[Mo_6O_{18}(AMBTH)]$ (top).

Crystal structure of **7**: Orange crystals of **7** were grown from a concentrated solution in DMSO kept in open air. Compound **7** crystallises in the $P\bar{1}$ space group (Figure 5). The diazoalkane ligand displays the characteristic features of the singly bent coordination mode with a linear Mo-N-N arrangement (angle of 176.6(5)°) and short Mo–N and N–N bond lengths (1.778(5) and 1.319(7) Å, respectively) indicative of multiple-bond character. Such a coordination mode is commonly observed in relatively high valent diazoalkane molybdenum complexes. The bonding parameters are close to those for $[Mo_6O_{18}(N_2CMeC_6H_4OMe)]^{2-}$[41] and are best described by a hybrid of resonance structures **a** and **b**.

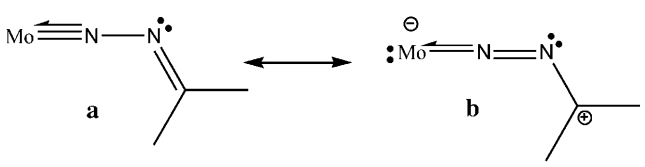

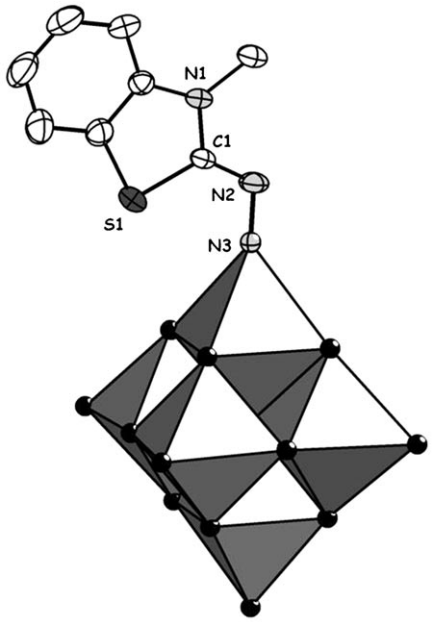

Figure 5. Molecular structure of $[Mo_6O_{18}(MBTH)]^{2-}$ (**7a**) in **7**.

The mercaptobenzothiazole moiety lies approximately in the bisecting plane of two $\{Mo_4O_4\}$ rings. The Mo–O distance between the functionalised Mo centre and the central oxygen atom O_c is at 2.194(3) Å significantly shorter than other Mo–O_c distances ranging from 2.358(3) to 2.394(3) Å. Analogous contractions have been observed in other monofunctionalised Lindqvist-type hexamolybdates, for example, diazenido, hydrazido and imido derivatives. This reflects the weaker *trans* influence of diazenido, hydrazido, imido and diazoalkane ligands compared to the oxo ligand.

NMR spectroscopy: Besides the characteristic peaks of the tetrabutylammonium cations, the ^{1}H NMR spectrum of **7** (Figure S2 in the Supporting Information) in [D_6]DMSO displays one singlet at $\delta = 3.58$ ppm and three multiplets in the aromatic region. Although the singlet can unambiguously be attributed to the NCH_3 of the thiazole ring, the aromatic region differs notably from that of the parent MBTH–H_2 spectrum. Indeed, the latter displays the expected pattern of two doublets of doublets and two triplets of doublets (J_3 values ≈ 8 Hz, J_4 values ≈ 1 Hz). In the functionalised polyanion, accidental overlapping of the resonances of two aromatic protons, as attested by the integration ratio (1:2:1), led to unusual patterns probably a result of second-order interactions, hard to analyze in term of coupling constants. The ^{13}C spectrum ([D_6]DMSO, see Figure S4 in the Supporting Information) displays the expected 12 signals. The $\delta =$ 8.6 ppm downfield shift of the C=N signal from the MBTH–H_2 to the $(NBu_4)_2$ $[Mo_6O_{19}$MBTH], clearly too large to be only attributed to the change of deuterated solvent ($CDCl_3$ vs. [D_6]DMSO), conveys the strong electronic withdrawing effect of the inorganic moiety, through the diazo bridge. Finally, the relative integration in ^{1}H NMR is in agreement with two tetrabutylammonium cations per benzothiazole moiety, as expected for a monofunctionalised polyanion.

The ^{1}H NMR spectra of $(NBu_4)_2[Mo_6O_{18}$(AMBTH)] and the hydrazone **5** (see Figure S5 and S6 in the Supporting Information) clearly show resolved signals that can be unambiguously assigned. The two aromatic protons of the central ring of the AMBTH ligand exhibit downfield chemical shifts compared with their chemical shifts in the parent monohydrazone, whereas the four aromatic protons of the terminal part are almost unchanged. In the ^{13}C{^{1}H} NMR spectrum of $(NBu_4)_2[Mo_6O_{18}$(AMBTH)] (see Figure S8 in the Supporting Information), the carbon bearing the hydrazone group also exhibits a downfield chemical shift compared to the parent hydrazone **5**, as was observed in the case of the MBTH–H_2/**7** couple. All these observations are again consistent with the electron-withdrawing effect of the hexamolybdate moiety. Finally, the relative integration is again consistent with two cations per benzothiazole moiety, as expected for a monosubstitution on the polyanion.

UV/Vis spectroscopy: The electronic properties of both $(NBu_4)_2[Mo_6O_{18}$(MBTH)] and $(NBu_4)_2[Mo_6O_{18}$(AMBTH)] were studied by UV/Vis absorption measurements (Figure 6 and Table 5). In both cases, the individual components only exhibit features in the UV part of the spectrum, below $\lambda =$ 400 nm. In $[Mo_6O_{19}]^{2-}$, the two observed bands at $\lambda = 262$ and 324 nm in DMSO, are attributed to O-to-Mo LMCT.[19] In the benzothiazole derivatives, absorption mainly arises from the $\pi \rightarrow \pi^*$ transitions. A very intense additional band is observed at $\lambda = 407$ nm for **7a** and at $\lambda = 443$ nm for **6a**. Interestingly, simple mixtures of the benzothiazole hydrazone and $(NBu_4)_2[Mo_6O_{19}]$ do not show such a feature, which confirms covalent linking in **6a** and **7a**. Such a strong electronic interaction between the polyoxometalate cluster and the functionalising organic moiety has already been observed and is attributed to an intramolecular charge-transfer transition from the organic donor to the POM-subunit.[56–57;61–62]

Table 5. UV/Vis spectroscopic data for $(NBu_4)_2[Mo_6O_{19}]$, MBTH-H_2, **5**, **6** and **7**.

	λ [nm], (ε [L mol^{-1} cm^{-1}])
$(NBu_4)_2[Mo_6O_{19}]$	262 (14700); 324 (6680)
MBTH–H_2	275 (7200); 313 (5800)
$(NBu_4)_2[Mo_6O_{18}$(MBTH)] (**7**)	283 (28500); 313 (sh,23000); 407 (24000)
AMBTH–H_2 (**5**)	301 (sh,10400); 340 (23500); 370 (40100)
$(NBu_4)_2[Mo_6O_{18}$(AMBTH)] (**6**)	307 (38100); 347 (48500); 357 (48000); 443 (36900)

Electrochemistry: The cyclic voltammogram of AMBTH–H_2 and MBTH–H_2 only displays irreversible oxidation process-

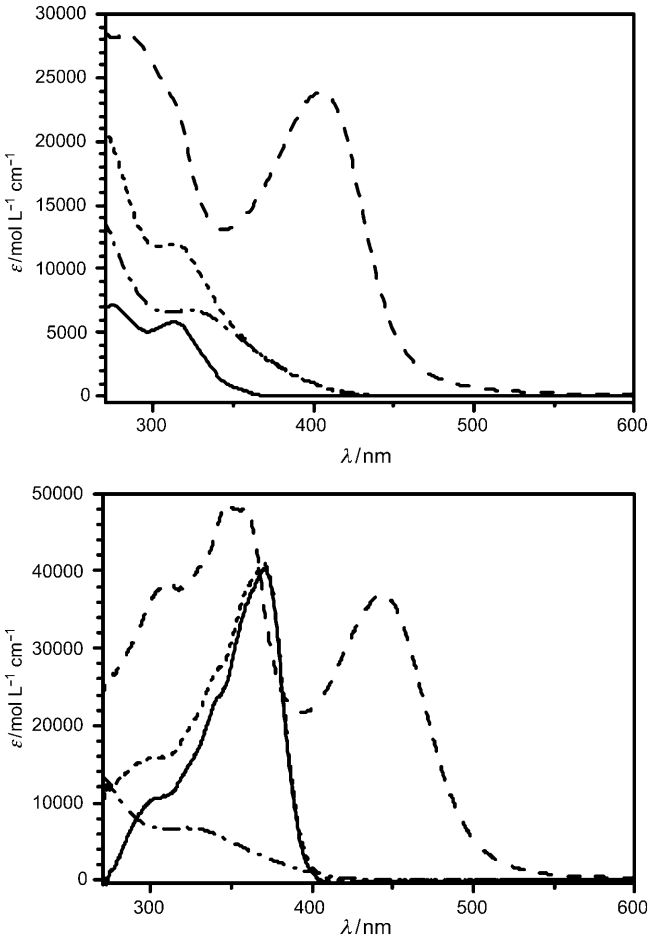

Figure 6. UV/Vis absorption spectra in DMSO. Top: MBTH-H_2 (——), $(NBu_4)_2[Mo_6O_{19}]$ (–•–•), 1/1 mixture of MBTH-H_2 and $(NBu_4)_2[Mo_6O_{19}]$ (•••••) and $(NBu_4)_2[Mo_6O_{18}(MBTH)]$ (-----); bottom: AMBTH-H_2 (——), $(NBu_4)_2[Mo_6O_{19}]$ (–•–•), 1/1 mixture of AMBTH–H_2 and $(NBu_4)_2[Mo_6O_{19}]$ (•••••) and $(NBu_4)_2[Mo_6O_{18}(AMBTH)]$ (-----).

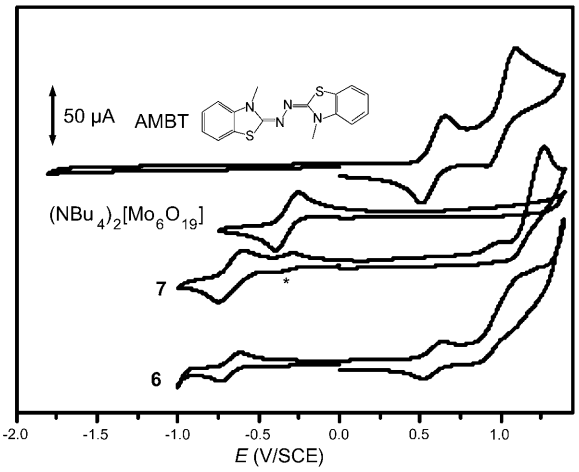

Figure 7. Cyclic voltammograms in DMSO/$(NBu_4)BF_4$ (0,1 M), scan rate 100 mV s,$^{-1}$ glassy carbon working electrode, Pt auxiliary electrode, SCE. From top to bottom: AMBT, $(NBu_4)_2[Mo_6O_{19}]$, $(NBu_4)_2[Mo_6O_{18}(MBTH)]$, $(NBu_4)_2[Mo_6O_{18}(AMBTH)]$. * : traces of $[Mo_6O_{19}]^{2-}$ in **7**.

es, probably due to hydrazone decomposition. For comparison purposes, we thus used the original AMBT as a reference for the organic part (Table 6). The cyclic voltammograms (CVs) of AMBT, $(NBu_4)_2[Mo_6O_{19}]$, $(NBu_4)_2[Mo_6O_{18}(MBTH)]$ (**7**) and $(NBu_4)_2[Mo_6O_{18}(AMBTH)]$ (**6**) in DMSO are displayed in Figure 7. The CV of AMBT shows two quasi-reversible one-electron oxidation processes at 0.582 and 1.003 V, corresponding to the successive formation of the radical cation and then the dication, as observed in acetonitrile.[63] On the other hand, $[Mo_6O_{19}]^{2-}$ undergoes a quasi-reversible reduction process at −0.325 V. A second reduction process may be observed for $[Mo_6O_{19}]^{2-}$, but it is irreversible in DMSO. The CVs of both $[Mo_6O_{18}(MBTH)]^{2-}$ and $[Mo_6O_{18}(AMBTH)]^{2-}$ show a quasi reversible reduction wave at about −0.67 V. The 0.35 V negative shift with respect to $[Mo_6O_{19}]^{2-}$ reflects the strong electron-donating properties of the diazoalkane ligand.

For the oxidation process, only irreversible features are observed for $[Mo_6O_{18}(MBTH)]^{2-}$, whereas $[Mo_6O_{18}(AMBTH)]^{2-}$ displays two fairly well-resolved processes. The first process, which is quasi-reversible, is assigned to the one-electron oxidation of the AMBTH component to give a radical cation. The shift with respect to the first oxidation process of AMBT is surprisingly small, which indicates that the expected negative shift owed to the negative charge of the hybrid is counterbalanced by the decrease in the electron density on the organic moiety as a result of strong donation to the inorganic component. Though it is not fully reversible, the second oxidation process can be correlated with the second wave of free AMBT.

Table 6. Electrochemical data.[a]

Compound	E_{pa}[b]	E_{pc}[b]	$^1/_2(E_{pa}+E_{pc})$[b]	$E_{pa}-E_{pc}$[c]
AMBT	0.656	0.508	0.582	148
	1.095	0.911	1.003	184
$(NBu_4)_2[Mo_6O_{19}]$	−0.253	−0.397	−0.325	144
$(NBu_4)_2[Mo_6O_{18}(MBTH)]$ (**7**)	−0.598	−0.748	−0.673	150
	0.18[d]			
	1.26[d]			
$(NBu_4)_2[Mo_6O_{18}(AMBTH)]$ (**6**)	−0.618	−7.36	−0.677	118
	0.645	0.521	0.583	124
	1.14	0.88	1.02	260
	1.24[d]			

[a] Glassy carbon electrode, $c = 10^{-3}$ mol L^{-1} in DMSO for AMBT and $(NBu_4)_2[Mo_6O_{19}]$, saturated DMSO solutions for **6** and **7**, 0.1 mol L^{-1} $(NBu_4)BF_4$, 100 mV s^{-1}. [b] V vs. SCE. [c] mV. [d] Irreversible.

Conclusion

The hydrazone AMBTH–H_2, a new member of the AMBT family, was synthesised in a five-step procedure and characterised by using single-crystal X-ray diffraction. In addition, the crystal structure of the re-

lated compound MBTH–H_2 and those of two intermediates in the synthesis of AMBTH–H_2 were determined. Coupling of MBTH–H_2 and AMBTH–H_2 to $[Mo_6O_{19}]^{2-}$ afforded two new diazoalkane–hexamolybdates isolated as tetrabutylammonium salts. The latter were characterised by using IR, UV/Vis and NMR spectroscopy, cyclic voltammetry, and in the case of the MBTH–hexamolybdate hybrid, single crystal X-ray diffraction. The packing arrangement of the molecules in crystals of AMBTH–H_2, the redox features of the AMBTH–hexamolybdate hybrid together with a good electronic communication between the organic π system and the molybdenum centres make these compounds very promising building blocks for the synthesis of conducting molecular materials. Electrocrystallisation of the hexamolybdate hybrids in the presence of AMBT or other organic donors (TTFs, perylene…) is underway to study the extent of interaction between the functionalised POM and the cationic donor. This strategy will be extended to Keggin- and Dawson-type POMs with emphasis on magnetic species. In parallel, the coordination chemistry of electroactive benzothiazole hydrazones will be developed. Electrocrystallisation of the resulting complexes might lead to materials with a good electronic interaction between the d/f electrons on the metal ions and the π system.[64,65]

Experimental Section

Materials and methods: Reagents and solvents were obtained from commercial sources and used as received unless otherwise stated. $(NBu_4)_2[Mo_6O_{19}]$ was synthesised according to literature procedure.[66] Reagent-grade acetonitrile was dried over calcium hydride before distillation. ^1H (300.13 MHz) and $^{13}C\{^1H\}$ (75.5 MHz) NMR spectra were recorded at 300 K in 5 mm o.d. tube by using a Bruker AC 300 spectrometer equipped with a QNP probehead. IR spectra were recorded from KBr pellets by using a Biorad FT 165 spectrometer. The electronic absorption spectra were recorded by using a Jasco V-670 spectrometer. Each compound was dissolved in DMSO at a concentration of 10^{-4} M. Cyclic voltammetry at a carbon electrode was carried out by using the EG&G model 273 A system. A standard three-electrode cell was used, which consisted of a glassy carbon working electrode, an auxiliary platinum electrode, and an aqueous saturated calomel electrode (SCE) equipped with a double junction. The scan rate was 100 mV s^{-1}. Each studied product was dissolved in DMSO (distilled and dried over 4 Å molecular sieves) with $(NBu_4)BF_4$ as electrolyte (0.1 M). Uncorrected fusion points were determined by using a Kofler bench. The ESI-MS spectra were acquired by using a triple quadrupole mass spectrometer API 3000 (Applied Biosystems, PE Sciex) in positive- and negative-ion mode. In positive-ion mode, the instrumental parameters were as follows: Nebulising gas N_2, 8 units flow rate; ion spray voltage, 5000 or 5500 V; temperature, room temperature; declustering potential, 20 V; focusing potential, 200 V; entrance potential, −10 V. In negative-ion mode, the instrumental parameters were as follows: nebulising gas N_2, 8 units flow rate; ion spray voltage, −5000 V; temperature, room temperature; declustering potential, −20 V; focusing potential, −200 V; entrance potential, 10 V. The experiments were performed by direct infusion with a syringe pump with a flow rate of 5–15 μL min^{-1}. ESI-MS samples were dissolved in DMSO and then diluted (10 times) in acetonitrile.

X-ray crystallographic data collection and refinement of structures: Yellow tabula of MBTH-H_2, yellow prisms of **2**, yellow plate-like crystals of **4**, red blocks of **5** and orange crystals of **7** were selected, mounted onto glass fibres, and transferred in a cold nitrogen gas stream. Intensity data were collected by using a Bruker-Nonius Kappa-CCD with graphite-monochromated Mo-Kα radiation. Unit-cell parameters determination, data collection strategy and integration were carried out by using the Nonius EVAL-14 suite of programs.[67] Multi-scan absorption correction was applied.[68] The structures were solved by direct methods using SHELXS-97 and refined anisotropically by full-matrix least-squares methods using the SHELXL-97 software package.[69] All non hydrogen atoms were refined anisotropically. Hydrogen atoms were introduced in calculated positions and their coordinates were refined with an overall isotropic thermal parameter. CCDC-766125 (MBTH–H_2), CCDC-766126 (**7**), CCDC-766127 (**2**), CCDC-766128 (**4**), CCDC-766129 (**5**) contain the supplementary crystallographic data for this paper. These data can be obtained free of charge from The Cambridge Crystallographic Data Centre via www.ccdc.cam.ac.uk/data_request/cif.

Syntheses

MBTH–H_2: This compound was synthesised according to the Riemschneider two-step procedure.[70] The first step was modified following Sutoris et al.[71] The product was recrystallised from EtOH as tabula X-ray quality crystals. ^1H NMR ($CDCl_3$): $\delta = 7.36$ (dd, $^3J(H,H) = 7.7$ Hz, $^4J(H,H) = 1.1$ Hz,1 H; ArH), 7.23 (td, $^3J(H,H) = 7.7$ Hz, $^4J(H,H) = 1.1$ Hz, 1 H; ArH), 6.96 (td, $^3J(H,H) = 7.7$ Hz, $^4J(H,H) = 1.1$ Hz, 1 H; ArH), 6.86 (d, $^3J(H,H) = 8$ Hz, 1 H; ArH), 4.24 (br, 2 H; NH_2), 3.39 ppm (s, 3 H; NCH_3); $^{13}C\{^1H\}$ NMR ($CDCl_3$): $\delta = 161.3$ (C=N), 142.9 (C_{qAr}), 127.3 (C_{ArH}), 124.3 (C_{qAr}), 123.3 (C_{ArH}), 121.5 (C_{ArH}), 109.2 (C_{ArH}), 31.4 ppm (NCH_3); IR (KBr): $\tilde{\nu} = 3283$ (s,ν_{NH}), 3173 (m), 3056 (w), 1655 (vs), 1585 (sh), 1576 (s), 1481 (s), 1456 (m), 1356 (sh), 1338 (s), 1307 (m), 1284 (w), 1253 (m), 1128 (m), 1077 (m), 1051 (m), 1027 (m), 1016 (m), 932 (m), 914 (sh), 842 (w), 734 (s), 717 (m), 682 (w), 616 (w), 597 (m), 524 (w), 495 (w), 429 cm^{-1} (w).

*Compound **1***: This compound was synthesised in quantitative yield according to Grandolini.[42] ^1H NMR ([D_6]DMSO): $\delta = 7.34$ (s, 1 H; ArH), 7.18 ppm (s, 1 H; ArH); $^{13}C\{^1H\}$ NMR ([D_6]DMSO): $\delta = 189.9$ (s, *C*=S), 140.9 (s, C_{Ar}), 126.0 (s, C_{Ar}), 114.1 (s, C_{Ar}), 96.1 ppm (s, C_{Ar}); IR (KBr): $\tilde{\nu} = 377$, 460, 549, 657, 686, 832, 1037, 1051, 1243, 1274, 1332, 1435, 1477, 1498, 1608, 1685, 2858, 2899, 3018, 3091 cm^{-1}.

*Compound **2***: This product was synthesised according to Grandolini,[42] then recrystallised from DMF. Yield: 44 %, Fp 250 °C. IR (KBr): $\tilde{\nu} = 303$, 359, 466, 700, 742, 853, 879, 971, 989, 1004, 1019, 1111, 1154, 1314, 1405, 1418, 1459, 1465, 1527, 2926 cm^{-1}. Yellow prismatic single crystals suitable for X-ray analysis were obtained by recrystallisation from a DMF solution.

*Compound **3***: This compound was synthesised by modification of a reported procedure.[43] Compound 2 (0.45 g, 1.6 mmol) was treated with Me_2SO_4 (2.40 mL, 25 mmol). The mixture was placed in a Teflon-lined Parr-acid-digestion bomb at 160 °C for 90 min and then cooled to room temperature. Water (5 mL) and KPF_6 (1.45 g, 7.9 mmol) were added, leading to the precipitation of a brown solid, which was separated by filtration, washed successively five times with water and five times with EtOAc, and then dried. Yield: 833 mg (87 %). ^1H NMR ([D_6]DMSO): $\delta = 9.31$ (s, 1 H; ArH), 8.98 (s, 1 H; ArH), 4.22 (s, 1 H; NCH_3), 3.19 ppm (s, 1 H; SCH_3); $^{13}C\{^1H\}$ NMR ([D_6]DMSO): $\delta = 185.6$ (s, *C*SMe), 142,9 (s, C_{Ar}), 127,1 (s, C_{Ar}), 119.4 (s, C_{Ar}), 102,8 (s, C_{Ar}), 37.0 (s, N*C*H_3), 18,2 ppm (s, S*C*H_3); IR (KBr): $\tilde{\nu} = 403$, 558 (ν_4P−F), 837 (ν_3P−F), 1035, 1093, 1111, 1172, 3050, 3150 cm^{-1}.

*Compound **4***: Compound **3** (0.80 g, 1.3 mmol) was treated with MBTH-H_2 (0.29 g, 1.6 mmol) in DMF (10 mL). After 16 h at room temperature, the orange suspension was filtered and the filtrate was evaporated to dryness to yield an orange solid residue. Then, this residue was dissolved in DMF (ca. 5 mL) and Et_2O (30 mL) was added to precipitate **4**. Yield: 691 mg (88 %). ^1H NMR ([D_6]DMSO): $\delta = 8.31$ (s, 1 H; ArH), 7.68 (s, 1 H; ArH), 7.42 (d, $^3J(H,H) = 9$ Hz, 1 H; ArH), 7.24 (t, $^3J(H,H) = 9$ Hz, 1 H; ArH), 7.03 (d, $^3J(H,H) = 9$ Hz, 1 H; ArH), 6.96 (t, $^3J(H,H) = 9$ Hz, 1 H; ArH), 3.91 (s, 3 H; NCH_3), 3.52 (s, 3 H; NCH_3), 3.38 (s, 3 H; NCH_3), 3.01 (s, 3 H; SCH_3); $^{13}C\{^1H\}$ NMR ([D_6]DMSO): $\delta = 178.6$ (s, *C*SMe), 158.9 (s, *C*=N), 156.5 (s, *C*=N), 143.2 (s, C_{Ar}), 141.8 (s, C_{Ar}), 140.9 (s, C_{Ar}), 126.2 (s, C_{Ar}), 125.2 (s, C_{Ar}), 122.9 (s, C_{Ar}), 121.9 (s, C_{Ar}), 120.9 (s, C_{Ar}), 120.2 (s, C_{Ar}), 116.1 (s, C_{Ar}), 108.9 (s, C_{Ar}), 94.76 (s, C_{Ar}), 38.7 (s, N*C*H_3), 31.1 (s, N*C*H_3), 30.3 ppm (s, N*C*H_3); IR (KBr): $\tilde{\nu} = 408$, 488, 535, 557, 751, 837, 950, 1023, 1090, 1158, 1257, 1304, 1361, 1396, 1422, 1476, 1579, 1600,

1619, 1655, 2919 cm^{-1}. Yellow plate-like single crystals suitable for X-ray analysis were obtained by slow evaporation at room temperature of a nitrobenzene solution.

*AMBTH–H_2 (**5**)*: To a solution of hydrazine (1.1 mL, 11.7 mmol, 10 eq) in DMF (5 mL) was added a solution of **4** (690 mg, 1.2 mmol) in DMF (5 mL), leading to the precipitation of a white solid. After 16 h at room temperature, the precipitate was separated by filtration, washed with water (3 × 10 mL) and then dried. Yield: 250 mg (50%). ^{1}H NMR ([D$_6$]DMSO): δ = 7.59 (s, 1H; ArH), 7.51 (d, ^3J(H,H) = 9 Hz, 1H; ArH), 7.27 (t, ^3J(H,H) = 9 Hz, 1H; ArH), 7.13 (d, ^3J(H,H) = 9 Hz, 1H; ArH), 7.00 (t, ^3J(H,H) = 6 Hz, 1H; ArH), 6.91 (s, 1H; ArH), 3.50 (s, 1H; NCH$_3$), 3.46 (s, 1H; NCH$_3$), 3.38 ppm (s, 1H; NCH$_3$); ^{13}C{^{1}H} NMR ([D$_6$]DMSO): δ = 156.6 (s, C=N), 141.3 (s, C_{Ar}), 141.0 (s, C_{Ar}), 140.5 (s, C_{Ar}), 126.3 (s, C_{Ar}), 123.1 (s, C_{Ar}), 122.2 (s, C_{Ar}), 120.7 (s, C_{Ar}), 115.5 (s, C_{Ar}), 114.4 (s, C_{Ar}), 113.9 (s, C_{Ar}), 109.1 (s, C_{Ar}), 91.1 (s, C_{Ar}), 30.5 (s, N*C*H$_3$), 30.4 ppm (s, N*C*H$_3$). One N-CH$_3$ and two C=N's carbons could not be detected, probably due to overlapping with the residual DMF peaks or slow relaxation. IR (KBr): $\tilde{\nu}$ = 482, 490, 535, 556, 573, 626, 659, 677, 717, 745, 765, 800, 864, 876, 916, 930, 960, 1020, 1035, 1087, 1116, 1133, 1148, 1253, 1296, 1341, 1357, 1376, 1395, 1420, 1458, 1478, 1509, 1576, 1601, 1621, 1656, 2981, 3069, 3309 cm^{-1}; ESI-MS : *m/z* (%): 428 (59) [*M*H$^+$], 855 (11) [*M*$_2$H$^+$]; Monocrystals suitable for X-ray analysis were obtained at room temperature from a nitrobenzene solution.

*(NBu$_4$)$_2$[Mo$_6$O$_{18}$(AMBTH)] (**6**)*: To a mixture of dicyclohexycarbodiimide (DCC, 105 mg, 0.51 mmol), 4-dimethylaminopyridine (DMAP, 17.5 mg, 0.14 mmol) and (NBu$_4$)$_2$[Mo$_6$O$_{19}$] (638 mg, 0.47 mmol) in distilled acetonitrile (5 mL) was added the monohydrazone **5** (200 mg, 0.47 mmol) under nitrogen atmosphere. After 18 h at reflux, the warm brown resulting suspension was filtered and the filtrate was stripped down. The residue was washed five times with 10 mL of methanol to remove residual dicyclohexylurea (DCU) (no remaining NH band at $\tilde{\nu}$ = 3331 cm^{-1} in the IR spectrum of the sample). Yield: 391 mg (47%). ^{1}H NMR ([D$_6$]DMSO): δ = 7.97 (s, 1H; ArH), 7.48 (d, ^3J(H,H) = 6 Hz, 1H; ArH), 7.25 (t, ^3J(H,H) = 6 Hz, 1H; ArH), 7.20 (s, 1H; ArH), 7.09 (d, ^3J(H,H) = 9 Hz, 1H; ArH), 6.98 (t, ^3J(H,H) = 9 Hz, 1H; ArH), 3.51 (s, 1H; NCH$_3$), 3.49 (s, 1H; NCH$_3$), 3.42 (s, 1H; NCH$_3$), 3.18 (t, ^3J(H,H) = 6 Hz, 16H; NCH$_2$), 1.58 (quintuplet, 7 Hz, ^3J(H,H) = 16H; N-CH$_2$-C*H*$_2$), 1.32 (sextuplet, ^3J(H,H) = 9 Hz, 16H; N-CH$_2$-CH$_2$-C*H*$_2$), 0.94 ppm (t, ^3J(H,H) = 7 Hz, 24H; N-CH$_2$-CH$_2$-CH$_2$-C*H*$_3$); ^{13}C{^{1}H} NMR ([D$_6$]DMSO): δ = 169.8 (s, C=N), 158.1 (s, C=N), 157.4 (s, C=N), 141.5 (s, Cq_{Ar}), 141.1 (s, Cq_{Ar}), 139.2 (s, Cq_{Ar}), 126.3 (s, CH_{Ar}), 123.0 (s, Cq_{Ar}), 122.0 (s, CH_{Ar}), 120.8 (s, CH_{Ar}), 119.5 (s, Cq_{Ar}), 116.0 (s, CH_{Ar}), 114.5 (s, Cq_{Ar}), 109.9 (s, CH_{Ar}), 93.6 (s, CH_{Ar}), 57.6 (s, N*C*H$_2$), 31.6 (s, N*C*H$_3$), 30.9 (s, N*C*H$_3$), 30.3 (s, N*C*H$_3$), 30.5 (s, N*C*H$_3$), 30.4 (s, N*C*H$_2$), 23.1 (s, NCH$_2$*C*H$_2$), 19.2 (s, NCH$_2$CH$_2$*C*H$_2$), 13.5 ppm (s, NCH$_2$CH$_2$CH$_2$*C*H$_3$); IR (KBr): $\tilde{\nu}$ = 470, 488, 531, 580, 629, 669, 696, 716, 767, 792, 867, 947, 972, 1024, 1054, 1091, 1120, 1216, 1291, 1343, 1359, 1383, 1408, 1474, 1508, 1580, 1597, 1611, 1647, 2873, 2936, 2960 cm^{-1}; UV/Vis (DMSO): λ_{max} (ε) = 357.5 (4.81×10^4), 443 nm (3.69×10^4 mol^{-1} dm^3 cm^{-1}); ESI-MS: *m/z* (%): 645.6 (63) [[Mo$_6$O$_{18}$(AMBTH)]$^{2-}$]. The presence of protonated 4-dimethylaminopyridine was detected by ESI-MS (DMAPH$^+$: *m/z* 123), ^{1}H NMR and ^{13}C NMR spectroscopy. ^{1}H NMR ([D$_6$]DMSO): δ = 8.18 (d, 2H; 6 Hz, Ar-*H*), 7.01 ppm (d, 2H; 6 Hz, Ar-*H*), N-CH$_3$ signals of the protonated DMAP may be overlapping with the N-CH$_2$ signals of the TBA. ^{13}C{^{1}H} NMR ([D$_6$]DMSO): δ = 156.8 (s, Cq_{Ar}), 138.2 (s, CH_{Ar}), 106.9 ppm (s, CH_{Ar}).

*(NBu$_4$)$_2$[Mo$_6$O$_{18}$(MBTH)] (**7**)*: To a yellow suspension of DCC (114 mg, 0.55 mmol, 1.1 equiv), DMAP (20 mg, 0.15 mmol, 0.3 equiv) and (NBu$_4$)$_2$[Mo$_6$O$_{19}$] (682 mg, 0.5 mmol, 1 equiv) in distilled dry acetonitrile (10 mL) was added MBTH-H$_2$ (90 mg, 0.5 mmol, 1 equiv) under nitrogen atmosphere, leading to an orange suspension. After one night at reflux, the dark brown hot suspension was filtered to remove most of the DCU. The crude filtrate was evaporated and the brown material was washed with hot MeOH (3 × 5 mL) to remove the remaining DCU. Yield 536 mg (70%). ^{1}H NMR ([D$_6$]DMSO): δ = 7.95 (d, 5 Hz, 1H; ArH), 7.50 (pseudo-d, 4 Hz, 2H; ArH), 7.28 (m, 1H; ArH), 3.58 (s, 3H; NCH$_3$), 3.19 (m, 16H; NCH$_2$C), 1.59 (m, 16H; NCCH$_2$C), 1.33 (sext., 7.5 Hz, 16H; NCCCH$_2$), 0.94 (t, 7.5 Hz, 24H; NCCCCH$_3$); ^{13}C{^{1}H} NMR ([D$_6$]DMSO): δ = 169.9 (C$_q$, C=N), 139.1 (C$_{qAr}$), 127.4 (C$_{ArH}$), 123.8 (C$_{ArH}$), 123.2 (C$_{ArH}$), 122.9 (C$_{qAr}$), 112,39 (C$_{ArH}$), 57.6 (N*C*H$_2$C), 31.4 (NCH$_3$), 23.1 (NC*C*H$_2$), 19.2 (NCC*C*H$_2$), 13.5 ppm (NCCCC*C*H$_3$); IR (KBr): $\tilde{\nu}$ = 2962 (m), 2931 (w), 2875 (w), 1647 (w), 1515 (s), 1471 (s), 1413 (m), 1375 (w), 1345 (w), 1289 (w), 1247 (w), 973 (m), 947 (s), 886 (w), 792 (s), 773 (s), 699 (w), 458 cm^{-1} (w); ESI-MS: *m/z* (%): 521.7 (100%) [[Mo$_6$O$_{18}$(MBTH)]$^{2-}$]; elemental analysis calcd (%) for (NBu$_4$)$_2$[Mo$_6$O$_{18}$(MBTH)]·2MeOH ($C_{42}H_{87}Mo_6N_5O_{20}S$): C 31.73, H 5.52, N 4.40, Mo 36.21; found: C 31.97, H 5.32, N 4.89, Mo 35.85. X-ray quality single crystals were grown as orange-brown squares from a concentrated DMSO solution kept in open air.

[1] G. R. Whittell, I. Manners, *Adv. Mater.* **2007**, *19*, 3439–3468.
[2] J. Gao, H. Gu, B. Xu, *Acc. Chem. Res.* **2009**, *42*, 1097–1107.
[3] C. Faulmann, K. Jacob, S. Dorbes, S. Lampert, I. Malfant, M.-L. Doublet, L. Valade, J. A. Real, *Inorg. Chem.* **2007**, *46*, 8548–8559.
[4] N. Avarvari, J. D. Wallis, *J. Mater. Chem.* **2009**, *19*, 4061–4076.
[5] E. Coronado, P. Day, *Chem. Rev.* **2004**, *104*, 5419–5448.
[6] E. Coronado, J. Galán-Mascarós, R. , C. Gómez-García, J. A. Murcia-Martínez, *Chem. Eur. J.* **2006**, *12*, 3484–3492.
[7] E. Chelebaeva, J. Larionova, Y. Guari, R. A. S. Ferreira, L. D. Carlos, F. A. A. Paz, A. Trifonov, C. Guerin, *Inorg. Chem.* **2009**, *48*, 5983–5995.
[8] J. Long, L.-M. Chamoreau, C. Mathoniere, V. Marvaud, *Inorg. Chem.* **2008**, *47*, 22–24.
[9] A. Bleuzen, V. Marvaud, C. Mathoniere, B. Sieklucka, M. Verdaguer, *Inorg. Chem.* **2009**, *48*, 3453–3466.
[10] A. B. Gaspar, V. Ksenofontov, M. Seredyuk, P. Gütlich, *Coord. Chem. Rev.* **2005**, *249*, 2661–2676.
[11] C. Train, R. Gheorghe, V. Krstic, L. M. Chamoreau, N. S. Ovanesyan, G. Rikken, M. Gruselle, M. Verdaguer, *Nat. Mater.* **2008**, *7*, 729–734.
[12] H. Hiraga, H. Miyasaka, R. Clerac, M. Fourmigue, M. Yamashita, *Inorg. Chem.* **2009**, *48*, 2887–2898.
[13] D. Lorcy, N. Bellec, *Chem. Rev.* **2004**, *104*, 5185–5202.
[14] S. Hünig, H. Balli, H. Conrad, A. Schott, *Justus Liebig Ann. Chem.* **1964**, *676*, 36-&.
[15] R. C. Wheland, J. L. Gillson, *J. Am. Chem. Soc.* **1976**, *98*, 3916–3925.
[16] P. Batail, K. Boubekeur, M. Fourmigue, J. C. P. Gabriel, *Chem. Mater.* **1998**, *10*, 3005–3015.
[17] A. Denis, P. Palvadeau, P. Molinie, K. Boubekeur, *C. R. Acad. Sci. II C* **2001**, *4*, 913–916.
[18] A. Denis, P. Palvadeau, P. Molinié, O. Chauvet, K. Boubekeur, *Solid State Sci.* **2001**, *3*, 715–725.
[19] A. Denis, K. Boubekeur, P. Molinié, P. Léone, P. Palvadeau, *J. Mol. Struct.* **2004**, *689*, 25–32.
[20] Z. Casar, I. Leban, A. Majcen-le Marechal, L. Piekara-Sady, D. Lorcy, *C. R. Acad. Sci. Ser. IIc* **2009**, *12*, 1057–1065.
[21] M. T. Pope, *Heteropoly and Isopoly Oxometalates*, Springer, New York, **1983**.
[22] M. T. Pope in *Polyoxo Anions: Synthesis and Structure, Vol. 4* (Ed.: A. G. Wedd) Elsevier, Oxford, **2004**, pp. 635–678.
[23] D. L. Long, E. Burkholder, L. Cronin, *Chem. Soc. Rev.* **2007**, *36*, 105–121.
[24] M. K. Seery, L. Guerin, R. J. Forster, E. Gicquel, V. Hultgren, A. M. Bond, A. G. Wedd, T. E. Keyes, *J. Phys. Chem. A* **2004**, *108*, 7399–7405.
[25] M. Clemente-León, E. Coronado, C. L. Gomez-Garcia, C. Mingotaud, S. Ravaine, G. Romualdo-Torres, P. Delhaes, *Chem. Eur. J.* **2005**, *11*, 3979–3987.
[26] D. G. Kurth, *Sci. Technol. Adv. Mater.* **2008**, *9*, 014103.
[27] W. Qi, H. L. Li, L. X. Wu, *J. Phys. Chem. B* **2008**, *112*, 8257–8263.
[28] E. Coronado, C. J. Gomez-Garcia, *Chem. Rev.* **1998**, *98*, 273–296.
[29] L. Ouahab, S. Gohlen, S. Triki in *Polyoxometalate Chemistry From Topology via Self-Assembly to Applications* (Eds.: M. T. Pope, A. Mueller), Kluwer Academic, Dordrecht, **2001**, pp. 205–229.

[30] E. Coronado, C. Gimenez-Saiz, C. J. Gomez-Garcia, S. C. Capelli, *Angew. Chem.* **2004**, *116*, 3084–3087; *Angew. Chem. Int. Ed.* **2004**, *43*, 3022–3025.
[31] E. Coronado, C. Giménez-Saiz, C. J. Gómez-García, *Coord. Chem. Rev.* **2005**, *249*, 1776–1796.
[32] A. Proust, R. Thouvenot, P. Gouzerh, *Chem. Commun.* **2008**, 1837–1852.
[33] M. Bonchio, M. Carraro, G. Scorrano, A. Bagno, *Adv. Synth. Catal.* **2004**, *346*, 648–654.
[34] M. Lu, B. H. Xie, J. H. Kang, F. C. Chen, Y. Yang. Z. H. Peng, *Chem. Mater.* **2005**, *17*, 402–408.
[35] B. B. Xu, M. Lu, J. H. Kang, D. Wang, J. Brown, Z. H. Peng, *Chem. Mater.* **2005**, *17*, 2841–2851.
[36] T. He, J. L. He, M. Lu, B. Chen, H. Pang, W. F. Reus, W. M. Nolte, D. P. Nackashi, P. D. Franzon, J. M. Tour, *J. Am. Chem. Soc.* **2006**, *128*, 14537–14541.
[37] M. Lu, W. A. Nolte, T. He, D. A. Corley, J. M. Tour, *Chem. Mater.* **2009**, *21*, 442–446.
[38] F. Odobel, M. Severac, Y. Pellegrin, E. Blart, C. Fosse, C. Cannizzo, C. R. Mayer, K. J. Eliott, A. Harriman, *Chem. Eur. J.* **2009**, *15*, 3130–3138.
[39] Z. H. Peng, *Angew. Chem.* **2004**, *116*, 948–953; *Angew. Chem. Int. Ed.* **2004**, *43*, 930–935.
[40] Y. Wei, B. Xu, C. L. Barnes, Z. Peng, *J. Am. Chem. Soc.* **2001**, *123*, 4083–4084.
[41] H. Kwen, V. G. Young, E. A. Maatta, *Angew. Chem.* **1999**, *111*, 1215–1217; *Angew. Chem. Int. Ed.* **1999**, *38*, 1145–1146.
[42] G. Grandolini, *Gazz. Chim. Ital.* **1960**, *90*, 1221–1229.
[43] G. Manecke, J. Kautz, *Makromol. Chem.* **1973**, *172*, 1–18.
[44] M. C. Etter, *Acc. Chem. Res.* **1990**, *23*, 120–126.
[45] G. A. Jeffrey, *An Introduction to Hydrogen Bonging*, Oxford University Press, New York, **1997**.
[46] T.-C. Hsieh, J. Zubieta, *Polyhedron* **1986**, *5*, 1655–1657.
[47] P. Gouzerh, Y. Jeannin, A. Proust, F. Robert, *Angew. Chem.* **1989**, *101*, 1377–1378; *Angew. Chem. Int. Ed. Engl.* **1989**, *28*, 1363–1364.
[48] A. Proust, R. Thouvenot, F. Robert, P. Gouzerh, *Inorg. Chem.* **1993**, *32*, 5299–5304.
[49] A. Proust, R. Thouvenot, S.-G. Roh, J.-K. Yoo, P. Gouzerh, *Inorg. Chem.* **1995**, *34*, 4106–4112.
[50] H. Y. Kang, J. Zubieta, *J. Chem. Soc. Chem. Commun.* **1988**, 1192–193.
[51] S. Bank, S. Liu, S. N. Shaikh, X. Sun, J. Zubieta, P. D. Ellis, *Inorg. Chem.* **1988**, *27*, 3535–3543.
[52] C. Bustos, B. Hasenknopf, R. Thouvenot, J. Vaissermann, A. Proust, P. Gouzerh, *Eur. J. Inorg. Chem.* **2003**, 2757–2766.
[53] Y. H. Du, A. L. Rheingold, E. A. Maatta, *J. Am. Chem. Soc.* **1992**, *114*, 345–346.
[54] A. Proust, R. Thouvenot, M. Chaussade, F. Robert, P. Gouzerh, *Inorg. Chim. Acta* **1994**, *224*, 81–95.
[55] W. Clegg, R. J. Errington, K. A. Fraser, S. A. Holmes, A. Schäfer, *J. Chem. Soc. Chem. Commun.* **1995**, 455–456.
[56] J. B. Strong, G. P. A. Yap, R. Ostrander, L. Liable-Sands, A. L. Rheingold, R. Thouvenot, P. Gouzerh, E. A. Maatta, *J. Am. Chem. Soc.* **2000**, *122*, 639–649.
[57] B. Xu, Y. Wei, C. L. Barnes, Z. Peng, *Angew. Chem.* **2001**, *113*, 2353–2356; *Angew. Chem. Int. Ed.* **2001**, *40*, 2290–2292.
[58] J. Hao, Y. Xia, L. Wang, L. Ruhlmann, Y. Zhu, Q. Li, P. Yin, Y. Wei, H. Guo, *Angew. Chem.* **2008**, *120*, 2666–2670; *Angew. Chem. Int. Ed.* **2008**, *47*, 2626–2630.
[59] M. Hidai, Y. Mizobe, M. Sato, T. Kodama, Y. Uchida, *J. Am. Chem. Soc.* **1978**, *100*, 5740–5748.
[60] G. L. Hillhouse, B. L. Haymore, *J. Am. Chem. Soc.* **1982**, *104*, 1537–1548.
[61] M. Lu, Y. G. Wei, B. B. Xu, C. F. C. Cheung, Z. H. Peng, D. R. Powell, *Angew. Chem.* **2002**, *114*, 1636–1638; *Angew. Chem. Int. Ed.* **2002**, *41*, 1566–1568.
[62] I. Bar-Nahum, K. V. Narasimhulu, L. Weiner, R. Neumann, *Inorg. Chem.* **2005**, *44*, 4900–4902.
[63] R. C. Wheland, *J. Am. Chem. Soc.* **1976**, *98*, 3926–3930.
[64] F. Pointillart, O. Maury, Y. Le Gal, S. Golhen, O. Cador, L. Ouahab, *Inorg. Chem.* **2009**, *48*, 7421–7429.
[65] F. Pointillart, Y. Le Gal, S. Golhen, O. Cador, L. Ouahab, *Inorg. Chem.* **2008**, *47*, 9730–9732.
[66] N. H. Hur, W. G. Klemperer, R.-C. Wang, *Inorg. Synth.* **1990**, *27*, 77–78.
[67] A. J. M. Duisenberg, L. M. J. Kroon-Batenburg , A. M. M. Schreurs, *J. Appl. Crystallogr.* **2003**, *36*, 220.
[68] R. H. Blessing, *Acta Crystallogr. Sect. A* **1995**, *51*, 33.
[69] G. M. Sheldrick, *Acta Crystallogr. Sect. A* **2008**, *64*, 112–122.
[70] R. Riemschneider, *Monatsh. Chem.* **1958**, *89*, 683–684.
[71] V. Sutoris, A. Gaplovsky, V. Sekerka, *Chem. Papers* **1986**, *40*, 103–114.

Received: February 18, 2010
Published online: June 22, 2010

